Conf-9106196--1

CONF-9106196--1

DE91 013414

JIHIR JOINT INSTITUTE FOR HEAVY ION RESEARCH
HOLIFIELD HEAVY ION RESEARCH FACILITY
P.O. BOX 2008, OAK RIDGE, TN 37831

REFLECTION-ASYMMETRIC SHAPES IN ATOMIC NUCLEI

W. Nazarewicz[+]
Joint Institute for Heavy Ion Research
Holifield Heavy Ion Research Facility
P.O. Box 2008, Oak Ridge, Tennessee 37831, USA

[+] On leave of absence from Institute of Theoretical Physics, Warsaw University

Document no. 91-03

REFLECTION-ASYMMETRIC SHAPES IN ATOMIC NUCLEI

W. Nazarewicz*
Joint Institute for Heavy-Ion Research,
Holifield Heavy Ion Research Facility,
P.O. Box 2008, Oak Ridge, Tennessee 37831, U.S.A.

ABSTRACT

Can atomic nuclei be unstable with respect to deformations that break intrinsic parity? On the theoretical side calculations indicate the existence of stable octupole deformations. There is also vast supporting experimental evidence for the presence of very collective low-energy dipole and octupole modes. In this contribution, recent advances in the physics of nuclear reflection-asymmetric shapes are discussed in terms of underlying shell effects. Particular attention is given to the recently predicted octupole excitations at superdeformed shapes.

INTRODUCTION

Why can certain nuclei be described in terms of intrinsic shapes with parity-breaking static moments? At first glance such a violation of a very fundamental symmetry is astonishing since strong interactions do actually conserve parity. One has to bear in mind, however, that the description in terms of the *intrinsic system* automatically involves the symmetry breaking mechanism. Of course, the fundamental quantum numbers, such as angular momentum, parity, baryon number, etc., associated with the basic space-time symmetries, are conserved in the laboratory system. On the other hand, in the body-fixed system of a nucleus the many-body wave function is, usually, not an eigenstate of fundamental symmetry operators. From this viewpoint the concept of nuclear stable octupole deformation is analogous to the idea of permanently quadrupole-deformed nuclear shapes. Therefore, if one accepts the possibility of stable quadrupole deformation in the ground state of the even-even nucleus, one cannot reject the picture of nuclear shapes that do not conserve *intrinsic parity*.

Microscopically, the symmetry breaking mechanism is always associated with pairs of quantum-mechanical states that are (almost) degenerate in energy. In quantal systems such a hybridization leads to reduced stability and even an infinitely small perturbation of a degenerate system produces a final response in the system due to the rearrangement of many close states. For instance, quadrupole deformation can be immediately associated with the residual interaction acting between spherical single-particle states of the isotropic harmonic oscillator. Indeed, as soon as the Fermi level

*On leave from the Institute of Theoretical Physics, Warsaw University

enters the valence shell the (ℓ, j) degeneracy is removed by the quadrupole–quadrupole force and the nucleus becomes deformed.

An analogous coupling between intrinsic states of opposite parity is produced by the long-range octupole-octupole residual interaction. In some cases the mixing is so strong that the nucleus acquires stable octupole deformation in the body-fixed frame. For normally–deformed systems the condition for strong octupole coupling occurs for particle numbers associated with the maximum ΔN=1 interaction between the intruder subshell (ℓ, j) and the normal parity subshell $(\ell - 3, j - 3)$. The regions of nuclei with strong octupole correlations correspond to particle numbers near 34 ($g_{9/2} \leftrightarrow p_{3/2}$ coupling), 56 ($h_{11/2} \leftrightarrow d_{5/2}$ coupling), 88 ($i_{13/2} \leftrightarrow f_{7/2}$ coupling), and 134 ($j_{15/2} \leftrightarrow g_{9/2}$ coupling), i.e. the tendency towards octupole deformation occurs just above closed shells.

The main goal of this presentation is not to cover the whole field of nuclear octupole and dipole modes. For this we rather refer the reader to recent reviews.[1-7] Instead, I would like to emphasize selected aspects of octupole collectivity. In particular, I will discuss "hidden" symmetries of the anisotropic harmonic oscillator and their apparent consequences for the presence of superdeformed reflection–asymmetric shapes.

REFLECTION–ASYMMETRIC SHAPES AT LOW EXCITATION ENERGY

For the Ra-Th (Z∼88, N∼134) and Ba-Sm (Z∼56, N∼88) nuclei, the features of stable octupole deformation, namely low-lying negative-parity states, parity doublets, alternating parity bands with enhanced E1 transitions have been established (for a recent review see, e.g., ref. [7]).

Many mean-field calculations predict reflection instability for nuclei around ^{222}Th and ^{146}Ba. There are calculations based on the Nilsson-Strutinsky approach with folded-Yukawa and Woods-Saxon deformed potentials[8-14] as well as Hartree–Fock calculations based on the Skyrme or Gogny forces.[15-20] All these models yield similar results for stable octupole deformations, but give slightly different predictions for the height of the octupole barrier.

The calculated octupole minima are usually very shallow with octupole barriers varying between 0.5 and 2 MeV, depending on the model. Consequently, dynamic fluctuations are expected to play a significant role. Some attempts towards including dynamic corrections by means of parity projection or gaussian overlap approximation have been made in refs.[17-20]

Deformation selfconsistent cranking calculations confirm empirical results, i.e. the stability of octupole deformation increases at medium spins.[21-23] The enhancement of octupole strength with rotation is caused by (i) weaker pairing correlations for the octupole shape, which increase the moments of inertia, and (ii) by the octupole mixing between single-particle states of opposite parity approaching each other with frequency.

In the presence of low-lying octupole excitations a large E1 moment may arise in the intrinsic frame due to a shift between the centre of charge and the centre of mass. Such a dipole moment manifests itself by very enhanced electric dipole transitions between opposite parity members of quasi-molecular rotational bands. Many properties of low-lying E1 modes in the transitional nuclei near ^{146}Ba and ^{224}Th can be explained by the reflection-asymmetric deformed shell model theory based on the Strutinsky renormalisation procedure.[22,24-26] The calculations reproduce the systematic trends seen in the experimental data and the vanishing values of the intrinsic dipole moments, D_0, in certain nuclei. In particular, it has been demonstrated[26] that the macroscopic contribution to the intrinsic dipole moment based on the droplet model is very small for lanthanides and becomes important in actinide nuclei, thus providing a consistent

description of experimental data in both mass regions. This effect is partly related to the presence of the neutron-skin contribution to D_0. Recently, first attempts to calculate intrinsic dipole moments within the full selfconsistent theory have been made. Egido and Robledo used the parity-projected HF+BCS model with Gogny interaction to reproduce B(E1) rates in the Ra-Th [19] and Ba [20] nuclei. They obtained excellent agreement with experimental data. For more discussion related to the question of "collective" intrinsic dipole moments I refer the reader to contribution by P. Butler.[27]

The complex interplay between rotation and reflection-asymmetric and triaxial degrees of freedom is most pronounced in transitional nuclei, like ^{218}Ra or ^{148}Sm, which do not have well developed ground-state deformation but still exhibit "quasirotational" bands of alternating parity and large B(E1) rates. According to the calculations[22, 23] octupole instability in these nuclei persists up to very high rotational frequencies. Such a pattern with low quadrupole- and strong octupole- and dipole collectivity has recently been observed in ^{218}Ra (ref. [28]) and ^{148}Sm (ref. [29]).

Other candidates for the strong octupole–quadrupole coupling can be find in medium–mass nuclei. In the $A\sim70$ mass region the shell correction calculations[10] predict octupole softness only in the transitional isotopes of Zn-Se with $N\leq36$. A recent study of the nucleus ^{64}Ge [30] suggests that a coupling between reflection-asymmetric and triaxial degrees of freedom takes place in this exotic $N=Z$ system[†].

The nonaxial, $K\neq0$, octupole components should certainly play a significant role at nearly spherical shapes. Very good testing-grounds for investigation the coupling between octupole excitations and triaxiality are the nuclei around ^{96}Zr, see discussion in refs.[7, 32]

NUCLEAR SHELL STRUCTURE AND OCTUPOLE DEFORMATION

Since the normal–parity single–particle states form a pseudo–oscillator pattern reflecting the presence of the pseudo-SU(3) symmetry[33-36] one can argue that many properties of deformed and superdeformed states should reflect basic features of the harmonic oscillator. In this section I shall discuss some properties of the single-particle shell structure of a three-dimensional harmonic oscillator with frequencies in rational ratios (RHO). The RHO classification scheme leads to the geometrical "multicluster" picture of nuclear deformed shapes. This simplistic picture is strongly supported by the behaviour of the octupole shell–forces of the RHO and the presented results of microscopic calculations.

Quantum Numbers of the Rational Harmonic Oscillator

The RHO exhibits the strongest level degeneracy that results in an appearance of spherical and deformed magic gaps. The problem of unusual degeneracies of the single–particle levels in the RHO has been extensively discussed in the literature, see reviews [37, 38] and refs. therein.

The single-particle Hamiltonian of the three–dimensional oscillator potential is given by

$$\hat{H} = \frac{1}{2}\sum_{i=1}^{3}(p_i^2 + \omega_i^2 x_i^2) = \frac{1}{2}\sum_{i=1}^{3}\omega_i\{a_i, a_i^+\}, \qquad (1)$$

where we assume $M=1$, $\hbar=1$. The single-particle energies of (1) are

$$e_{n_1,n_2,n_3} = \sum_{i=1}^{3}\omega_i\left(n_i + \frac{1}{2}\right), \qquad (2)$$

[†]In the recent work[31] Skalski employed parameterisation of nuclear shapes involving both β_3 and γ and confirmed octupole instability and γ-softness in ^{64}Ge.

where n_i are numbers of oscillator quanta in three spatial directions. The single-particle diagram of the axially-deformed harmonic oscillator is displayed in fig. 1. Here

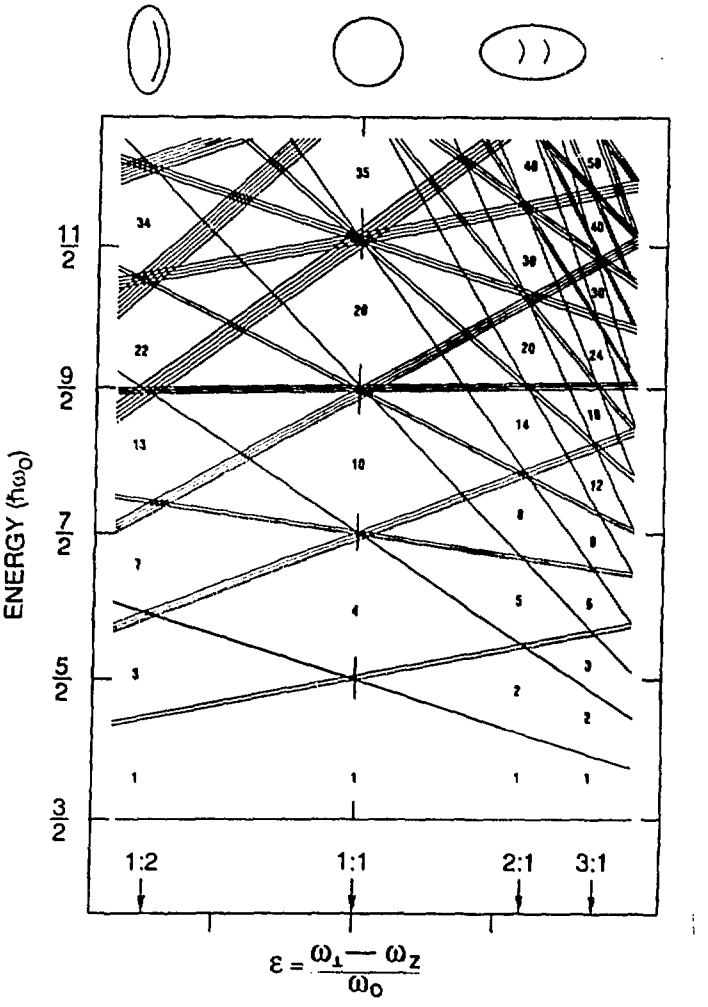

Fig. 1. Single-particle level spectrum of the axially symmetric harmonic oscillator shown as a function of quadrupole deformation ε. Here $\omega_o = \frac{1}{3}(2\omega_\perp + \omega_3)$. The orbital degeneracy is $n_\perp+1$, which is illustrated by artificially splitting the lines. The arrows indicate the characteristic deformations corresponding to the ratio of $\omega_\perp : \omega_3 =$ 1:2, 1:1, 2:1 and 3:1.

$\omega_1 = \omega_2 = \omega_\perp$ and the single-particle energies depend only on two quantum numbers: $n_\perp = n_1 + n_2$ and n_3. Due to the axial symmetry each level is $(n_\perp + 1)$ times degenerate.

For the *RHO* the ratios of frequencies are rational numbers. This condition can be expressed in terms of three integers k_i, i=1,2,3:

$$\omega_i k_i = \tilde{\omega}, \tag{3}$$

where $\tilde{\omega}$ can be calculated from the volume conservation condition, $\omega_1\omega_2\omega_3 = \tilde{\omega}_o^3$, and is equal to

$$\tilde{\omega} = \sqrt[3]{k_1 k_2 k_3} \cdot \tilde{\omega}_o, \quad \tilde{\omega}_o = \frac{41}{A^{1/3}}. \tag{4}$$

For example, the spherical shape corresponds to $k_1=k_2=k_3=1$, while the axial shapes have $k_1=k_2=k_\perp$. In the axial case it is convenient to write the single-particle energies in terms of the shell frequency, ω_{shell}, and the shell principal quantum, N_{shell}, defined by [39]:

$$\omega_\perp n_\perp + \omega_3 n_z = \omega_{shell} N_{shell}, \quad N_{shell} = n_\perp k_3 + n_3 k_\perp, \quad \omega_{shell} = \frac{\tilde{\omega}}{k_\perp k_3}. \tag{5}$$

Let us now introduce new quantum numbers ν_i and λ_i:

$$n_i = k_i \nu_i + \lambda_i, \qquad \nu_i = \left[\frac{n_i}{k_i}\right], \qquad \lambda_i = n_i \,(\mathrm{mod}\, k_i), \tag{6}$$

where the symbol $[x]$ stands for the integer part of x. Single-particle energies of the RHO can be thus written as

$$e_{M;\lambda_1\lambda_2\lambda_3} = \tilde{\omega} M + \tilde{\omega} \sum_{i=1}^{3} \frac{\lambda_i + \frac{1}{2}}{k_i}, \tag{7}$$

where $M = \nu_1 + \nu_2 + \nu_3$ is the new principal quantum number. At fixed values of λ_i the level degeneracy is equal to $\frac{1}{2}(M+1)(M+2)$, i.e. it corresponds exactly to the degeneracy of a spherical oscillator with principal quantum number M. In the next step one can introduce new ladder operators[40-42]

$$A_i^{\{\lambda\}} = \frac{1}{\sqrt{k_i}} (a_i)^{k_i} \left(\frac{\hat{n}_i - \lambda_i}{\hat{n}_i(\hat{n}_i - 1)...(\hat{n}_i - k_i + 1)} \right)^{\frac{1}{2}} = (a_i)^{k_i} \left(\left[\frac{\hat{n}_i}{k_i}\right] \frac{(\hat{n}_i - k_i)!}{\hat{n}_i!} \right)^{\frac{1}{2}}, \tag{8}$$

where $\hat{n}_i = a_i^+ a_i$ is the boson number operator and $\{\lambda\} \equiv \{\lambda_1\lambda_2\lambda_3\}$. It is easy to verify that operators (8) indeed fulfil the standard boson commutation rules, i.e.

$$\left[A_i^{\{\lambda\}}, A_j^{\{\lambda\}+}\right] = \delta_{i,j}. \tag{9}$$

The new boson operator $A_i^{\{\lambda\}}$ acts only on the quantum number ν_i *leaving* λ_i *unchanged*,

$$A_j^{\{\lambda\}+} | \cdots, \nu_i k_i + \lambda_i, \cdots \rangle = \sqrt{\nu_i + 1} | \cdots, (\nu_i + 1) k_i + \lambda_i, \cdots \rangle. \tag{10}$$

Now, analogously to the well-known spherical case, one can construct eight generators linear in $\left\{A_i^{\{\lambda\}}, A_i^{\{\lambda\}+}\right\}$ that fulfil the commutation rules of SU(3) and commute with the RHO Hamiltonian. This proves that the dynamical symmetry in question is SU(3). The RHO eigenstates belonging to the same $\{\lambda\}$ family form for a given M the basis of an irreducible symmetric representation (irrep) of SU(3), $(M, \{\lambda\})$. Each family has a corresponding ground state belonging to the one-dimensional representation of SU(3) for M=0, which is the vacuum for the new bosons, eq. (8). Since $0 \le \lambda_i < k_i$ the number of $\{\lambda\}$-families is equal to $k_1 k_2 k_3$.

At the spherical shape, $k_1=k_2=k_3=1$, there is only one family present, labelled by $\{\lambda\}=(000)$. The degeneracy of each level is $\frac{1}{2}(M+1)(M+2)$ and the magic gaps occur at particle numbers

$$N_M = \frac{1}{6}(M+1)(M+2)(M+3) = 1,\ 4,\ 10,\ 20,\ 35,\ 56,\ 84,\ \cdots \tag{11}$$

Other cases of significant physical interest are the superdeformed prolate (k_1=1, k_2=1, k_3=2) and the hyperdeformed prolate (k_1=1, k_2=1, k_3=3) shapes. Here, since

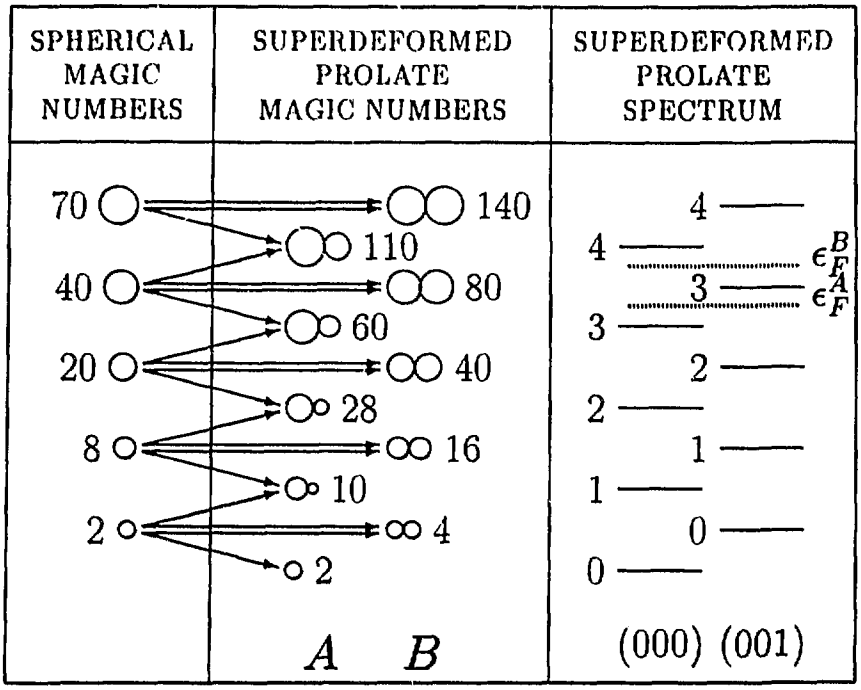

Fig. 2. Magic numbers and spectrum of the prolate superdeformed (k_1=1, k_2=1, k_3=2) harmonic oscillator. The arrows indicate from which spherical oscillator representations a given superdeformed representation is built (see text). The sizes of circles schematically illustrate the dimensions of spherical representations. The harmonic oscillator degeneracies have been doubled to take into account the spin. Two different positions of the Fermi level, ϵ_F^A and ϵ_F^B, are indicated in the spectrum. The quantum numbers $(\lambda_1, \lambda_2, \lambda_3)$ of two λ-families are shown below the spectrum. (Taken from ref. [38].)

λ_1=λ_2=0, the number of independent SU(3) irreps for a given M is equal simply to k_3 and they can be easily distinguished by means of λ_3.

As seen in fig. 2 there are two kinds of closed-shell systems that are expected at superdeformed shapes. In the "asymmetric" case, indicated as A, the number of filled shells within the family (λ)=(000) is larger by one than that within the family (λ)=(001). In fig. 2 this is illustrated by the position of the Fermi level ϵ_F^A. Consequently the magic numbers are then equal to sums of two consecutive spherical magic numbers and read $N_{M+1}^{(000)}+N_M^{(001)}$=1, 5, 14, 30, 55, etc. The numbers shown in the figure have been doubled to include the spin degeneracy. In the "symmetric" variant B the missing (001) shell is filled and the magic numbers are equal to doubled spherical oscillator magic numbers, $N_M^{(000)}+N_M^{(001)}$=2, 8, 20, 40, 70, etc.

The situation becomes slightly more complex at hyperdeformed shapes, see fig. 3. In the "strongly asymmetric" variant A the number of filled shells within the family (000) is larger by one than those of the families (001) and (002), which leads to magic numbers $N_{M+1}^{000}+N_M^{001}+N_M^{002}$=1, 6, 18, 40, 75, etc. In the variant B the occupation of the family (002) is lower than those of the families (000) and (001) and the resulting magic

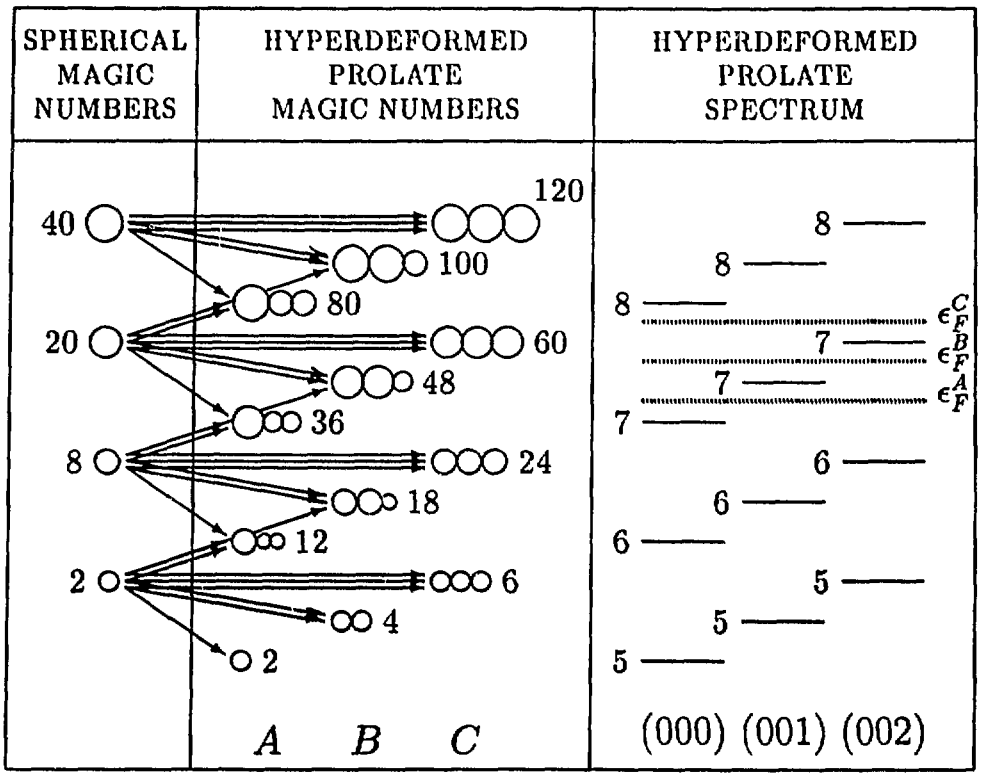

Fig. 3. Similar to fig. 2 but for the prolate hyperdeformed (k_1=1, k_2=1, k_3=3) harmonic oscillator. Three different positions of the Fermi level, ϵ_F^A, ϵ_F^B, and ϵ_F^C, are indicated in the spectrum. The quantum numbers ($\lambda_1\lambda_2\lambda_3$) of three λ-families are shown below the spectrum. (Taken from ref. [38].)

numbers are $N_{Nl+1}^{000}+N_{Nl+1}^{001}+N_{Nl}^{002}$=2, 9, 24, 50, 90, etc. Finally, in the "symmetric" case C the occupations of families (000), (001) and (002) are identical and the magic numbers are equal to tripled spherical oscillator magic numbers, $N_{Nl}^{000}+N_{Nl}^{001}+N_{Nl}^{002}$=3, 12, 30, 60 and 105, etc.

The examples discussed so far represent the simplest possible situation in which the numbers k_i are relatively prime. The degeneracy pattern becomes, however, rather complicated in the case when two k_i's have a common multiplier. Such a situation is present where different irreps of SU(3) are degenerate, e.g., on the oblate side, k_1=k_2=$k_\perp$>1, k_3=1.

In order to label the oblate superdeformed shells of the RHO, one can introduce quantum numbers $\lambda_\perp$ and $\tilde{N}$ defined in a similar way as λ, (see e.g. ref.[43]):

$$\lambda_\perp = \nu_\perp \,(\mathrm{mod}\, k_\perp), \quad \tilde{N} = \nu_\perp + \nu_3, \tag{12}$$

where $\nu_\perp$=$[n_\perp/k_\perp]$. Contrary to the case of prolate shapes the shell degeneracy depends explicitly on $\lambda_\perp$:

$$n(\tilde{N},\lambda_\perp) = \frac{1}{2}(\tilde{N}+1)[k_\perp\tilde{N} + 2(\lambda_\perp+1)]. \tag{13}$$

It can be shown (see detailed discussion in ref.[38]) that (i) the degeneracy pattern of the RHO on the oblate side represented by labelling (12) corresponds in fact to reducible representations of SU(3) [44], and (ii) in the particular case of superdeformed oblate nuclei, $k_\perp$=2, k_3=1, the dynamical symmetry is O(4) [45].

Multicluster Model

According to eq. (5) the energy difference between neighbouring oscillator shells, $\tilde{\omega}_{shell}$, decreases smoothly with deformation. This indicates that the overall magnitude of the shell effects is expected to be strongest at the spherical shape. Below are discussed some examples that indicate that even at very strong elongations the appearing shell structure leads to an enhanced stability similar to that observed for spherical shell gaps. Moreover, we will describe the deformed shell-stabilized systems in terms of "multiclusters" of spherical subsystems (clusters), as dictated by the decomposition of the RHO representations into the isotropic ones, as described in the previous section. Of course, the term "cluster" should not be understood in the most direct sense of a spatial spherical cluster, since in medium mass and heavy nuclei the probability of clustering into large fragments is strongly inhibited by the Pauli principle. However, it turns out that the group-theory symmetries of these clusters induce some properties of superdeformed states as if the clustering occurred in the real space.

> The main assumption of the "cluster" model is that every $\{\lambda\}$-family (an SU(3) oscillator) should correspond to an independent fragment. The number of fragments is then equal to the number of one-dimensional irreps of SU(3), i.e. it is equal to $k_1k_2k_3$.

Octupole Shell Force of the RHO

The degenerate shell of the RHO consists, in general, of states having different parities. Indeed, the generalized Bose operators (8) are parity–even for even values of k_i and parity–odd for odd values of k_i. Consequently, the total parity of single–particle state $|\hat{n}\rangle=|n_1n_2n_3\rangle$ can be written as

$$\pi_{\hat{n}} = (-1)^N = (-1)^{\lambda_1+\lambda_2+\lambda_3}(-1)^{k_1\nu_1+k_2\nu_2+k_3\nu_3} = \pi_\lambda\pi_\nu. \qquad (14)$$

The above expression can be given a simple interpretation. The parity π_λ is the intrinsic parity of the corresponding bosonic vacuum whilst π_ν represents the parity of an excited mode. In the case of superdeformed prolate shapes with even values of k_3, eq. (14) reduces to

$$\pi_{\hat{n}} = (-1)^{\lambda_3}(-1)^{n_\perp} = (-1)^{\lambda_3+\Lambda}, \qquad (15)$$

where Λ is the projection of the orbital angular momentum on the symmetry axis (z-axis).

The fact that degenerate single–particle orbitals have different parities has interesting consequences for the octupole mode, $Q_{3K}=r^3Y_{3K}$, since the optimum condition for the level hybridization is met. Table 1 shows the energies of particle–hole excitations associated with various components of octupole tensor. Let us first consider the superdeformed shape with $k_\perp$=1 and k_3=2. The K=1 and K=3 octupole components conserve intrinsic parity π_λ. Interestingly, since $\Delta E=2\omega_3-\omega_\perp=0$, for K=1 there exist non–vanishing matrix elements between states belonging to the same supershell. This suggests that superdeformed magic prolate nuclei are potential candidates for stable

Table 1. Energies of the particle-hole excitation, ΔE, associated with the octupole interaction Q_{3K}.

K	$\Delta E/\hbar$	Optimal conditions for instability
0	ω_3, $2\omega_\perp$-ω_3, $2\omega_\perp$+ω_3, $3\omega_3$	superdeformed oblate shapes
1	$\omega_\perp$, $2\omega_3$-$\omega_\perp$, $2\omega_3$+$\omega_\perp$, $3\omega_\perp$	superdeformed prolate shapes
2	ω_3, $2\omega_\perp$-ω_3, $2\omega_\perp$+ω_3	superdeformed oblate shapes
3	$\omega_\perp$, $3\omega_\perp$	no instability

"banana shapes" [46, 47], $K=1$ octupole deformations[‡]. The $K=0$ and $K=2$ interactions act only between states with opposite values of π_λ. At the superdeformed oblate shape with $k_\perp=2$, $k_3=1$, this scenario is reversed: the $K=0$ and $K=2$ modes conserve π_λ. By inspecting Table 1 one can immediately conclude that the superdeformed oblate nuclei should be unstable with respect to $K=0$ and $K=2$ octupole fields ($\Delta E=2\omega_\perp-\omega_3=0$!).

In order to analyze the octupole couplings in the RHO model, the doubly-stretched octupole interaction,

$$Q''_{3K} = r''^3 Y_{3K}(\Omega''), \qquad x''_i \equiv \frac{\omega_i}{\omega_0} x_i, \ (i=1,2,3) \tag{16}$$

of Sakamoto and Kishimoto [48, 49] has been used. This interaction can be viewed as an improved conventional multipole-multipole force. Firstly, it satisfies the nuclear-selfconsistency[§] rigorously even if the system is deformed. Secondly, it yields the zero-energy RPA spurious modes, i.e. it automatically separates the translational and reorientation modes. Last but not least, for the doubly-stretched interaction the coupling between octupole and dipole modes disappears.

Let us first discuss properties of low-lying octupole modes within the RPA formalism. The RPA equation for the excitation energy, ω, is given by the dispersion relation

$$\frac{1}{\kappa^{scif}_{3K}} - R_{3K}(\omega) = 0, \tag{17}$$

where κ^{scif}_{3K} is the self-consistent octupole coupling strength[48],

$$\begin{aligned} \frac{4\pi M\omega_0^2}{7\kappa^{scif}_{3K}} &= \langle (r^4)'' \rangle_0 + \frac{2}{7}(4-K^2)\langle (r^4 P_2)'' \rangle_0 \\ &+ \frac{1}{84}\left[K^2(7K^2-67)+72\right]\langle (r^4 P_4)'' \rangle_0, \end{aligned} \tag{18}$$

and

$$R_{3K}(\omega) = \sum_i \frac{E_i - E_0}{(E_i-E_0)^2-\omega^2}\left[|\langle i|Q''_{3K}|0\rangle|^2 + |\langle i|Q''^*_{3K}|0\rangle|^2\right] \tag{19}$$

is the RPA response function. The value of $R_{3K}(\omega=0)/2$ is the inverse energy-weighted sum rule S_{-1}, which can be related to the *microscopic* interaction strength, κ^{mic}_{3K}, by [50]

$$\kappa^{mic}_{3K} = (2S_{-1})^{-1}. \tag{20}$$

[‡]Strictly speaking the instability is not expected for doubly magic systems since the corresponding coupling disappears. The optimal situation is expected to occur in nuclei that are singly magic. In this case the superdeformed shape is stabilized by the magic neutron/proton gap whilst the instability is caused by valence protons/neutrons.

[§]The shape of the potential and that of the density must be the same [39].

Consequently, if the quantity

$$I_{3K} \equiv (\kappa_{3K}^{self})^{-1} - (\kappa_{3K}^{mic})^{-1} \tag{21}$$

is negative (positive), then the lowest energy octupole mode is unstable (stable) with respect to permanent deformation. In order to check the susceptibility of the RHO to octupole distortions one can thus calculate I_{3K} as a function of the shell filling. For the RHO this can be done analytically. Below are presented selected result of the calculations for the K=0 mode (and closed-shell systems).

(i) **Spherical case,** $k_1=k_2=k_3=1$. Here

$$I_{30}^{sph} = \frac{7}{4\pi}\frac{1}{\omega_0^4}A\frac{5}{2} > 0, \tag{22}$$

where $A=N_M$ is the particle number, cf. eq. (11), and M is the principal quantum number of the last occupied shell. It is seen that the spherical magic harmonic oscillator is *stable* with respect to octupole distortion and I_{30} does not exhibit any shell fluctuations[¶].

(ii) **Superdeformed case,** $k_1=k_2=1$, $k_3=2$. Here, the result depends on the value of N_{shell}, i.e.

$$I_{30}^{SD} = \frac{7}{40\pi}\frac{\omega_3^2}{\omega_0^6}A \times \begin{cases} 37 & \text{asymmetric system, case } A \text{ of fig. 2} \\ 73 & \text{symmetric system, case } B \text{ of fig. 2.} \end{cases} \tag{23}$$

(iii) **Hyperdeformed case,** $k_1=k_2=1$, $k_3=3$. Here we consider three positions of the Fermi level, see fig. 3. Also in this case the result depends on N_{shell}:

$$I_{30}^{HD} = \frac{7}{1120\pi}\frac{\omega_3^2}{\omega_0^6}A \times \begin{cases} 2252\left(1-\frac{0.58}{M+2}\right) & \text{asymmetric system, } \epsilon_F^A \\ 2252\left(1+\frac{0.58}{M+2}\right) & \text{asymmetric system, } \epsilon_F^B \\ 4316 & \text{symmetric system, } \epsilon_F^C. \end{cases} \tag{24}$$

As seen from eqs. (23-24) there exists a correlation between the predictions of the geometrical multi-cluster model and the underlying single-particle picture. Namely, for the systems expected to be asymmetric the value of I_{30} is small, and it increases for more symmetric multicluster configurations. This result is already quite encouraging. However, no octupole instability has been predicted by the RPA since in all cases $I_{30}>0$. On the other hand, it is well known that the deformed shell model alone (here: the RHO) is not able to predict correctly the nuclear binding and deformation energies since it partly neglects the interaction energy arising from the two-body effective forces [50]. According to the Strutinsky energy theorem the fluctuating part of the total energy, the shell-correction, is, however, reproduced fairly well by the independent single-particle model.

Since we know that the smooth energy of the harmonic oscillator is a very poor approximation to the liquid drop energy we should not expect the RPA result discussed above to be very accurate[‖]. In the next step, therefore, we calculate the shell driving force associated with the doubly-stretched octupole interactions.

[¶]It is worth noting that the exact result (22) comes from from the delicate cancelation between the M-dependent terms. In ref. [48], where the the terms of $O(1/M^2)$ were neglected, the authors obtained I_{30}=0 also for spherical closed-shell systems.

[‖]The RPA is the harmonic expansion around the equilibrium point and its predictions depend crucially on the curvature of the total potential energy.

In the presence of the small perturbing potential, V, the total shell correction can be written as

$$\delta E_{shell} = \delta E^{(0)}_{shell} + \delta E^{(1)}_{shell} + \delta E^{(2)}_{shell} + \ldots \tag{25}$$

where $\delta E^{(0)}_{shell}$ is the unperturbed shell correction,

$$\delta E^{(1)}_{shell} = \sum_{\alpha=1}^{A} V_{\alpha\alpha} - \sum_{\alpha=1}^{\infty} V_{\alpha\alpha}\tilde{n}_\alpha \tag{26}$$

is the first order correction to δE_{shell} [51], and

$$\delta E^{(2)}_{shell} = \sum_{\alpha=1}^{A}\sum_{\beta=A+1}^{\infty} \frac{|V_{\alpha\beta}|^2}{E_0 - E_{\alpha\beta}} - \sum_{\alpha=1}^{\infty}\sum_{\beta=1}^{\infty} \frac{|V_{\alpha\beta}|^2}{E_0 - E_{\alpha\beta}}(\tilde{n}_\alpha - \tilde{n}_\beta) \tag{27}$$

is the second order contribution to the shell energy. In eqs. (26-27) $\tilde{n}_\alpha$ is the smoothed occupation number of the single-particle state $|\alpha\rangle$ and $E_{\alpha\beta}$-E_0 is the particle-hole excitation energy.

For the octupole field, V=$\beta_{3K}Q''_{3K}$, the first order term (26) vanishes and the shell driving force is solely determined by the second order correction $\delta E^{(2)}_{shell}$, which is proportional to the square of the corresponding deformation β_{3K},

$$\delta E^{(2)}_{shell} = C_{3K}\beta^2_{3K}. \tag{28}$$

The shell-energy octupole-stiffness coefficient, C_{3K}, given by eq. (27) ($V \rightarrow Q''_{3K}$), determines the octupole susceptibility of shell energy. If C_{3K} is negative then there exists a shell force favouring stable deformations**. On the other hand, if C_{3K} is positive, the shell correction tends to restore reflection symmetry.

The results of calculations for C_{3K} are displayed in figs. 4-6. For the spherical shape, fig. 4, the octupole-driving shell force is positive, i.e. there is no tendency to develop stable octupole deformations. Of course, in this case all octupole modes are degenerate.

The situation at superdeformed prolate shape is shown in fig. 5. For particle numbers representing the asymmetric case A of fig. 2 (N_{shell}-even) the C_{3K} is negative for the K=0,1 and 3 modes. For the symmetric systems (case B) there is no shell octupole driving force towards reflection-asymmetric shapes.

Finally, the hyperdeformed case is illustrated in fig. 6. As expected, for the systems representing the asymmetric case A of fig. 3 the shell correction decreases with octupole deformations for the K=0,1 and 3 modes, whilst no octupole-driving tendency is predicted for the symmetric case C.

In summary, the role of spherical clusters in defining properties of superdeformed states becomes more clear when one considers the shell energy of the RHO. For magic numbers given by two unequal spherical clusters (case A in fig. 2, i.e., N or Z equal to 28, 60, 110 etc.), the shell energy decreases with increasing reflection asymmetry. On the other hand, for the particle numbers 40, 80, 140 (case B), the nuclear shape is expected to be fairly rigid with respect to reflection asymmetric distortions††. For hyperdeformed shapes, fig. 3, the harmonic oscillator model suggests that the strongest tendency for reflection asymmetry should be expected in case A, i.e. for the particle

**The liquid drop model energy never favours reflection-asymmetric shapes. This means that stable octupole shapes can only arise from shell effects, i.e. from the shell driving force.

††The relation between spherical and superdeformed magic numbers was discussed by Bengtsson et al. in 1981 [43]. In order to understand the alternating behaviour of microscopic octupole shell correction they introduced the model of two touching harmonic oscillators, i.e. two spherical clusters.

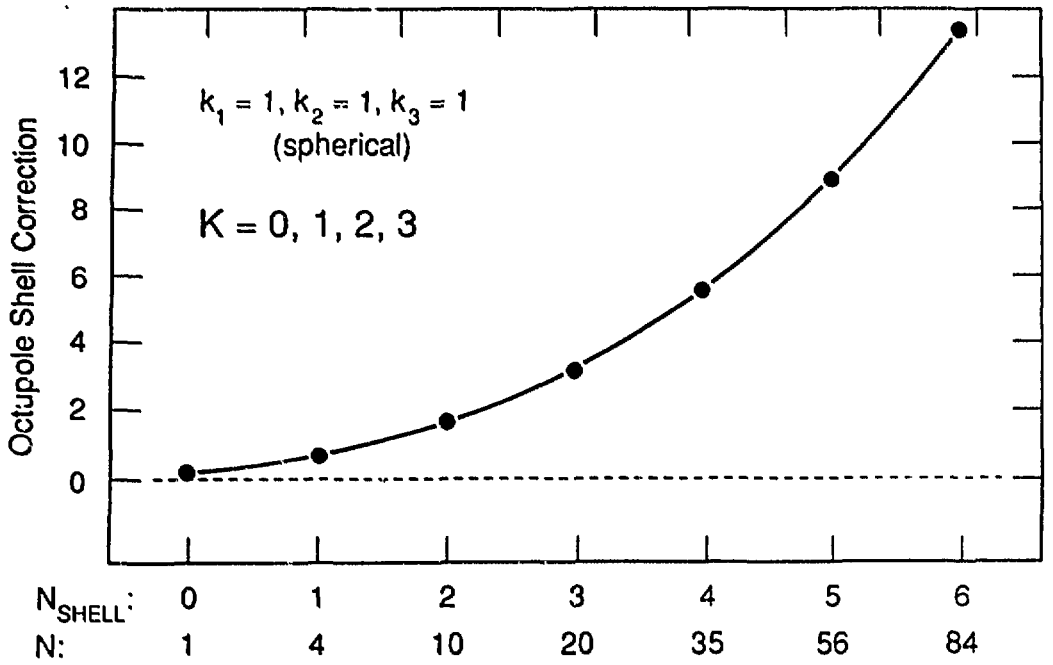

Fig. 4. Shell-correction octupole-stiffness coefficient C_{3K} (in units of $\frac{7}{4\pi}\tilde{\omega}_0^{-1}$ for the closed-shell configurations of the spherical harmonic oscillator.

numbers 12, 36, 80, 150. Particle numbers that stabilize reflection-symmetric shapes (case C) are equal to 24, 60, 120.

Reflection–Asymmetric Shapes in Light Nuclei

In light nuclei the spin–orbit interaction is relatively weak and, in addition, the diffuseness of the nuclear surface is comparable with the nuclear radius. Consequently, the harmonic oscillator model gives a fairly good approximation to the nuclear average potential. Among many well-deformed configurations in light nuclei there are several good examples that nicely illustrate the simple oscillator (multicluster) scheme.

A classic example is the ground-state of ^{20}Ne, which can be well described as arising from an ^{16}O–^{4}He di-nucleus configuration[52-54]. According to the RHO scheme this *reflection asymmetric superdeformed* system can be viewed as a combination of two spherical "clusters" with particle numbers 2 (alpha particle) and 8 (spherical ^{16}O).

There are several candidates for reflection-asymmetric structures among the so called quasi-molecular resonances. For instance, the alternating parity band built on the 0_2^+ state in ^{18}O can be well described in terms of α+^{14}C dipole molecular band [55]. Observed resonances in the asymmetric fission ^{24}Mg$\rightarrow^{16}$O + ^{8}Be (or ^{20}Ne+α) can be attributed to the calculated low-lying reflection-asymmetric hyperdeformed minimum in ^{24}Mg [56]. According to the RHO scheme this configuration can be associated with the symmetric α+^{16}O+α (see [57]) or asymmetric ^{16}O+α+α or ^{16}O+^{8}Be structures.

Octupole Correlations in Superdeformed Nuclei

The microscopic mechanism behind reflection asymmetry at certain superdeformed shapes is twofold. The octupole interaction Y_{30} couples the orbitals with asymptotic quantum numbers $[N\ n_z\ \Lambda]\Omega$ and $[N+1\ n_z \pm 1\ \Lambda]\Omega$. The largest number of such matrix elements corresponds to states with the highest possible value of $n_\perp$, i.e.

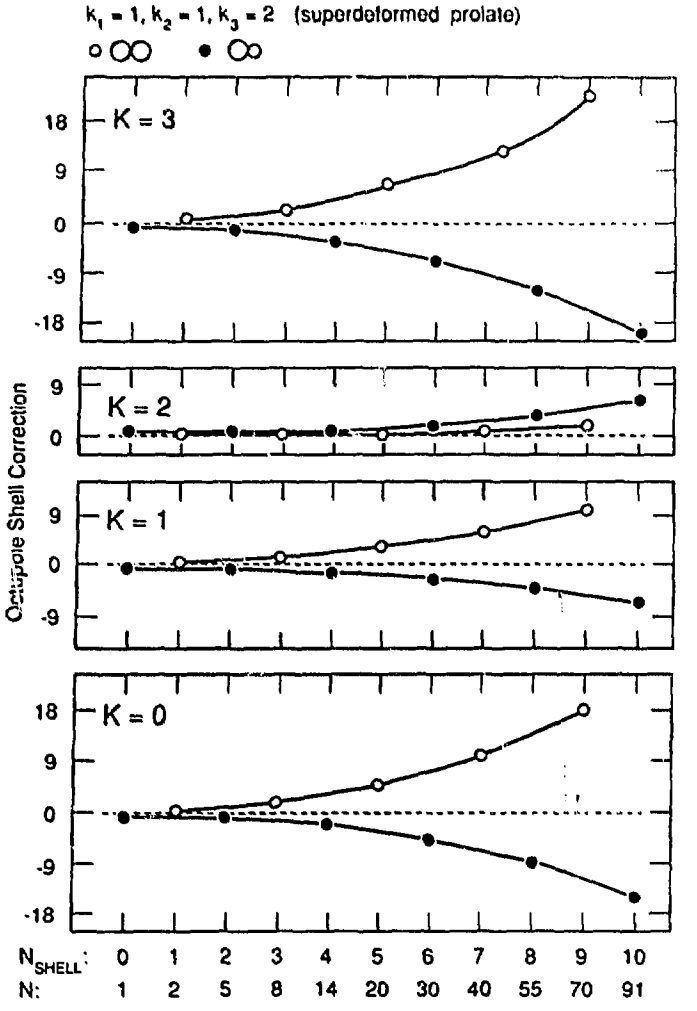

Fig. 5. Similar to fig. 4 but for the superdeformed closed-shell configurations of the RHO.

for n_3=0. This tendency has been discussed long ago in the context of the fission barrier asymmetry [58, 59]. The second mechanism behind the octupole instability in superdeformed states is the octupole interaction between the high-N intruder orbitals and specific pseudo-oscillator levels. For example, the same pairs of orbitals, such as ([660]1/2–[530]1/2) or ([770]1/2–[640]1/2), which are responsible for octupole deformations in the light actinides, appear close to the Fermi level in superdeformed SD configurations around ^{148}Gd and ^{192}Hg.

Calculations based on the realistic mean-field potentials confirm the prediction of the RHO, i.e. regions of particle numbers, which favour reflection-symmetric or reflection-asymmetric shapes alternate[43,60-63] and the tendency towards mass-asymmetry is strongly favoured at particle numbers around 28, 64 and 114 whilst for particle numbers around 38, 84 and 144 the minimum shell correction energy is found at reflection-symmetric shapes.

For superdeformed bands around ^{152}Dy the low-energy octupole collectivity can be attributed to the "octupole-driving" proton number Z=64. On the other hand

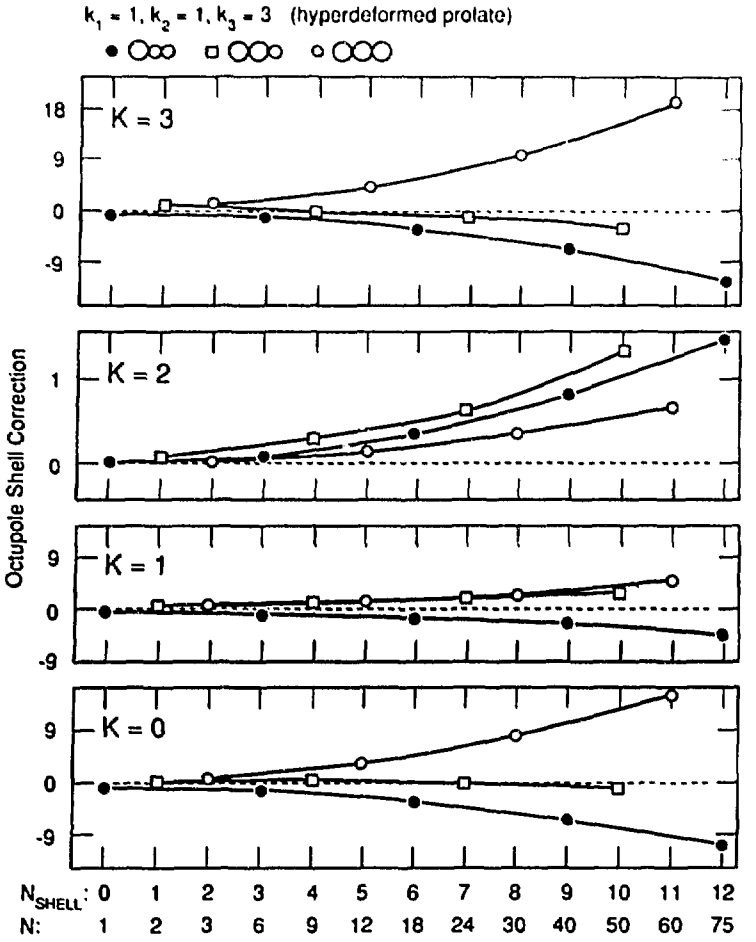

Fig. 6. Similar to fig. 4 but for the hyperdeformed closed-shell configurations of the RHO.

there is no such a tendency for the neutron system. But as predicted, the particle number N=84 has been found to strongly favour reflection-symmetric shapes. The opposite is true for superdeformed configurations in the Hg-Pb region, i.e. octupole correlations have neutron origin (because of the "optimal" neutron number N=114). As an illustrative example the results of Woods-Saxon-Strutinsky calculations for ^{192}Hg are shown in fig. 7. Whilst the neutron shell correction strongly favours octupole distortions the proton shell correction drives the system towards β_3=0. The resulting shell correction is almost insensitive to β_3 and, thanks to the very shallow macroscopic energy, the total potential energy reveals a pronounced octupole softness.

Recently, the octupole susceptibility in superdeformed configurations has been investigated within the parity-projected Skyrme-Hartree-Fock model [64]. The selfconsistent calculations do confirm the predictions of models based on the shell-correction approach, i.e. they indicate quite a sizeable lowering of the octupole excitations built on the superdeformed intrinsic state. Recent calculations [65] in terms of the Generator Coordinate Method (GCM) confirm this tendency.

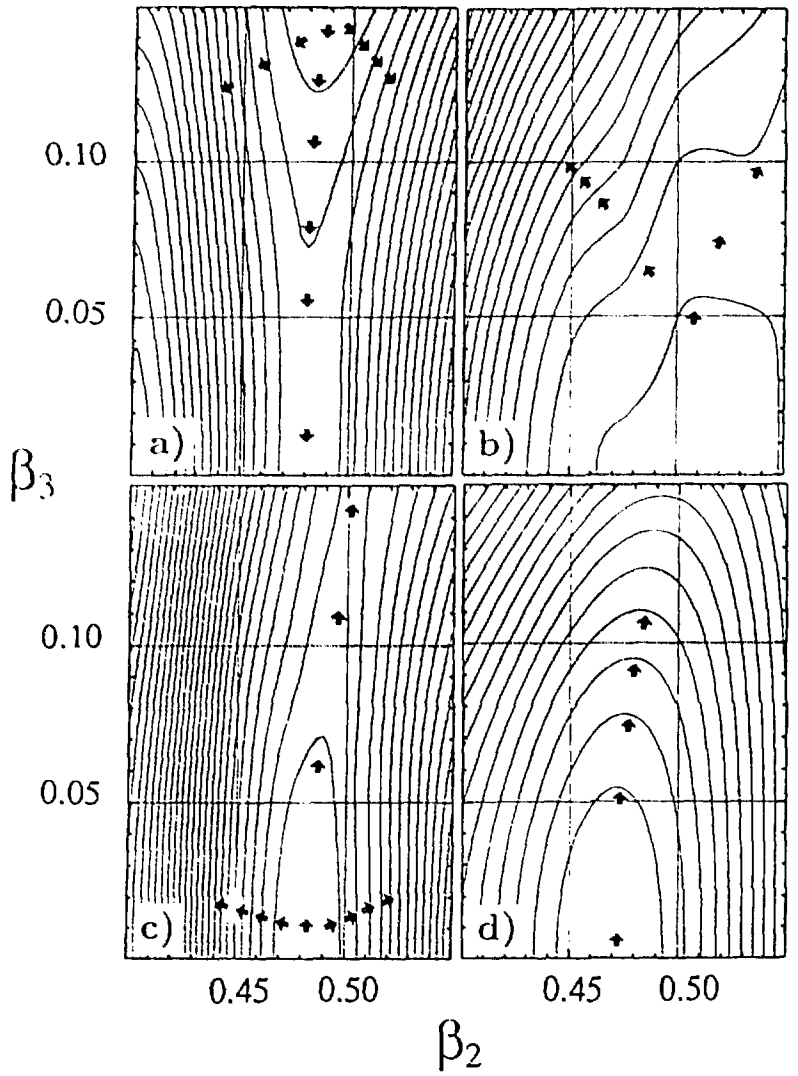

Fig. 7. The neutron shell correction energy (a), the proton shell correction energy (b), the total shell energy (c) and the total potential energy (d) for ^{192}Hg as a function of β_2 and β_3. Arrows indicate the direction of growing energy. The distance between the contour lines is 200 keV. (From [62].)

Properties of low-frequency octupole vibrations built upon superdeformed shapes have been analysed recently by Mizutori et al. [47,66,67] in terms of the RPA method with the cranked Nilsson potential and the doubly-stretched octupole residual interaction. They found rather strong K-dependence of superdeformed octupole modes. In particular, the K=1 "banana" mode turned out to be very collective. At normal deformations, the spatial difference between doubly-stretched and normal multipole-multipole forces is rather small. At large deformations, however, these interactions give

markedly different predictions. For instance, the K=3 octupole vibrations are very collective in terms of doubly-stretched coordinates, but they are relatively weak when expressed through normal octupole interactions [67]. This means that the experimental observation (or: non-observation) of very collective K=3 octupole vibrations will tell us which of these two residual interactions is more realistic.

The deformation-driving shell-forces of K=0,1,2,3 superdeformed octupole modes have been recently discussed in ref. [68] within the deformed Woods-Saxon model. The calculations indicate a correlation between the shell forces of different K-modes. This result is in a qualitative agreement with the predictions of the RHO model.

Octupole softness (but not *octupole instability*) in superdeformed nuclei in the A$\sim$190 region is expected to persist at high angular momenta.[47,60,61,63,66,67]. Consequently, collective octupole vibrational excitations can be mixed with low-lying one- and two-particle states thus modifying the excitation pattern near the yrast line. According to the calculations the first excited state in the doubly-magic superdeformed configurations in ^{152}Dy and ^{192}Hg should have a collective octupole character, in a nice analogy to the well-known collective 3$^-$ state in the doubly-magic spherical nucleus ^{208}Pb. Moreover, the B(E1) rates for depopulating the superdeformed octupole band should be markedly enhanced because of (i) the reduced excitation energy of the giant dipole resonance built on the superdeformed state [25] and (ii) the large macroscopic contribution to the intrinsic dipole moment, which is proportional to the product of $\beta_2\beta_3$. The presence of large dipole moments (or enhanced B(E1) rates) is a direct consequence of the doubly-stretched octupole force. The K=0 and K=1 $(r^3Y_{3K})''$ operators are linear combinations of the ordinary octupole fields, r^3Y_{3K} and the compressional dipole fields, r^3Y_{1K} [67]. Again, if the doubly-stretched residual interaction is realised in nature, strong dipole transitions de-exciting superdeformed octupole states should be present.

Recent experimental data on ^{193}Hg [69] show a low-frequency pseudo crossing in one of the observed superdeformed bands as well as dipole transitions (most likely in one direction only) between one superdeformed band and another. An admixture of an octupole phonon built on the [624]9/2 ground-state into the [512]5/2 band provides a possible explanation of these effects [69]. The experimental data for ^{193}Hg, together with the observed reduction in alignments and the unusual similarity of superdeformed bands in the A$\sim$190 region, are the first pieces of experimental evidence supporting the presence of strong octupole correlations in superdeformed configurations.

As far as hyperdeformed shapes are concerned, a third hyperdeformed minimum around the fission barrier has been calculated [70-72] for neutron-rich nuclei around Z=86, N=148, i.e. exactly around the octupole-driving particle numbers 80 and 150). Experimentally, the third minimum shows up as an alternating-parity microstructure of resonances [73, 74].

SUMMARY

The field of octupole deformation is among the most quickly expanding areas of nuclear structure. Experimental discovery of nuclear quasimolecular bands, parity doublets and collective intrinsic dipole moments certainly gave this subject a strong push. Theoretically, many properties of low-lying octupole and dipole modes have been successfully described using reflection-asymmetric mean field approach and collective models like the GCM or RPA.

Recent discovery of discrete superdeformed rotational bands in heavy nuclei opened up a whole new field, namely the near yrast superdeformed spectroscopy. Especially exciting is the question of low-energy collective excitations at very deformed

configurations. Among them, the octupole modes have been predicted to be particularly favoured. In this contribution, overall features of octupole correlations have been described in terms of the RHO model. In particular, we have demonstrated that there exists an apparent relation between the multiple irreps of SU(3) and the tendency (susceptibility) to cluster into spherical fragments. The simple relation between the cluster size, the number of clusters (equal to the number of irreps of SU(3)), and the overall equilibrium shape is supported by the microscopic calculations.

Acknowledgements This work has been partly done in collaboration with J. Dobaczewski and P. Van Isacker. Useful discussions with K. Matsuyanagi and R. Robinson are gratefully acknowledged. The Joint Institute for Heavy Ion Research has as member institutions the University of Tennessee, Vanderbilt University, and the Oak Ridge National Laboratory; it is supported by the members and by the Department of Energy through Contract Number DE-FG05-87ER40361 with the University of Tennessee. This project was supported in part by the Polish Ministry of National Education under Contract G-MEN-147/90.

REFERENCES

1. G.A. Leander, *in*: "Nuclear Structure 1985", R.A. Broglia, G.B. Hagemann and B. Herskind, eds., North-Holland, Amsterdam (1985) p. 249.

2. W. Nazarewicz, *in*: "Nuclear Structure 1985", R.A. Broglia, G.B. Hagemann and B. Herskind, eds., North-Holland, Amsterdam (1985) p. 263.

3. J. Żylicz, *in*: "Nuclear Structure, Reaction and Symmetries", R.A. Meyer and V. Paar, eds., World Scientific, Singapore (1986) p. 79.

4. R.R. Chasman, *in*: "Nuclear Structure, Reaction and Symmetries", R.A. Meyer and V. Paar, eds., World Scientific, Singapore (1986) p. 5.

5. P. Butler, *in*: "Heavy Ions in Nuclear and Atomic Physics", Z. Wilhelmi and G. Szeflińska, eds., Adam Hilger, Bristol and Philadelphia (1989) p. 295.

6. S.G. Rohoziński, *Rep. Prog. Phys.* 51:541 (1988).

7. W. Nazarewicz, *Nucl. Phys.* A520:333c (1990).

8. P. Möller and J.R. Nix, *Nucl. Phys.* A361:117 (1981).

9. G.A. Leander, R.K. Sheline, P. Möller, P. Olanders, I. Ragnarsson and A.J. Sierk, *Nucl. Phys.* A388:452 (1982).

10. W. Nazarewicz, P. Olanders, I. Ragnarsson, J. Dudek, G.A. Leander, P. Möller and E. Ruchowska, *Nucl. Phys.* A429:269 (1984).

11. R.R. Chasman, *J. Physique* 45:C5 (1984).

12. A. Sobiczewski, Z. Patyk, S. Ćwiok and P. Rozmej, *Nucl. Phys.* A485:16 (1988).

13. S. Ćwiok and W. Nazarewicz, *Phys. Lett.* 224B:5 (1989).

14. S. Ćwiok and W. Nazarewicz, *Nucl. Phys.* A496:367 (1989); *Nucl. Phys.* A (1991) in press.

15. P. Bonche, P.H. Heenen, H. Flocard and D. Vautherin, *Phys. Lett.* 175B: 387 (1986).

16. L.M. Robledo, J.L. Egido, J.F. Berger and M. Girod, *Phys. Lett.* 187B:233 (1987).

17. P. Bonche, *in*: "The Variety of Nuclear Shapes", J.D. Garrett et al., eds., World Scientific, Singapore (1988) p.302.

18. L.M. Robledo, J.L. Egido, B. Nerlo-Pomorska and K. Pomorski, *Phys. Lett.* 201B:409 (1988).

19. J.L. Egido and L.M. Robledo, *Nucl. Phys.* A494:85 (1989).

20. J.L. Egido and L.M. Robledo, *Nucl. Phys.* A518:475 (1990).

21. W. Nazarewicz, P. Olanders, I. Ragnarsson, J. Dudek and G.A. Leander, *Phys. Rev. Lett.* 52:1272 (1984); 53:2060E (1984).

22. W. Nazarewicz, *in*: "Proc. Int. Conf. on Nuclear Structure Through Static and Dynamic Moments", H.H. Bolotin, ed., Conference Proceedings Press, Melbourne, (1987) p. 180.

23. W. Nazarewicz, G.A. Leander and J. Dudek, *Nucl. Phys.* A467:437 (1987).

24. G.A. Leander, *in*: "AIP Conf. Proc. 125", American Institute of Physics, New York (1985) p. 125.

25. G.A. Leander, W. Nazarewicz, G.F. Bertsch and J. Dudek, *Nucl. Phys.* A453:58 (1986).

26. P. Butler and W. Nazarewicz, submitted to *Nucl. Phys.* A.

27. P. Butler, these proceedings.

28. N. Schulz, V.R. Vanin, M. Aiche, A. Chevallier, J. Chevallier, J.C. Sens, Ch. Briançon, S. Ćwiok, E. Ruchowska, J. Fernandez-Niello, Ch. Mittag and J. Dudek, *Phys. Rev. Lett.* 63:2645 (1989).

29. W. Urban, R.M. Lieder, J.C. Bacelar, P.P. Singh, D. Alber, D. Balabanski, W. Gast, H. Grawe, G. Hebbinghaus, J.R. Jongman, T. Morek, R.F. Noorman, T. Rząca-Urban, H. Schnare, M. Thoms, O. Zell and W. Nazarewicz, *Phys. Lett.* B (1991), in press.

30. P.J. Ennis, C.J. Lister, W. Gelletly, H.G. Price, B.J. Varley, P.A. Butler, T. Hoare, S. Ćwiok and W. Nazarewicz, to be published.

31. J. Skalski, *Phys. Rev.* C43:140 (1991).

32. H. Mach, S. Ćwiok, W. Nazarewicz, B. Fogelberg, M. Moszyński, J. Winger and R.L. Gill, *Phys. Rev.* C42:R811 (1990).

33. R.D. Ratna-Raju, J.P. Draayer and K.T. Hecht, *Nucl. Phys.* A202:433 (1973).

34. A. Bohr, I. Hamamoto and B.R. Mottelson, *Phys. Scr.* 26:267 (1982).

35. J.P. Draayer, *Nucl. Phys.* A520:259c (1990).

36. J. Dudek, W. Nazarewicz, Z. Szymański and G.A. Leander, *Phys. Rev. Lett.* 59:1405 (1987).

37. H.V. McIntosh, *in*: "Group Theory and Its Applications", E.M Loebl, ed., Academic Press, New York and London (1971), vol. II, p.75.

38. W. Nazarewicz, J. Dobaczewski, P. Van Isacker, *in*: APS Proc. Press (1991), in press; Preprint JIHIR 91-02 (1991).

39. A. Bohr and B.R. Mottelson, "Nuclear Structure", vol. 2, W.A. Benjamin, New York (1975).

40. F. Duimio and G. Zambotti, *Nuovo Cimento* 48A: (1966) 1203.

41. I. Vendramin, *Nuovo Cimento*, 54A:190 (1968).

42. R.A. Brandt and O.W. Greenberg, *J. Math. Phys.* 10:1168 (1969).

43. T. Bengtsson, M.E. Faber, G. Leander, P. Möller, M. Ploszajczak, I. Ragnarsson and S. Åberg, *Phys. Scr.* 24:200 (1981).

44. G. Maiella and G. Vilasi, *Lett. Nuovo Cimento*, 1:57 (1969).

45. A. Cisneros and H.V. McIntosh, *J. Math. Phys.* 11:870 (1970).

46. B.R. Mottelson, Symp. on Nucl. Struc., Argonne 1988; Copenhagen Workshop 1988.

47. S. Mizutori, K. Matsuyanagi and Y.R. Shimizu, *in*: APS Proc. Press (1991), in press; preprint KUNS 1069 (1991).

48. H. Sakamoto and T. Kishimoto, *Nucl. Phys.* A501:205 (1989).

49. H. Sakamoto and T. Kishimoto, *Nucl. Phys.* A501:242 (1989).

50. P. Ring and P. Schuck, "The Nuclear Many-Body Problem", Springer-Verlag, New York (1980).

51. M. Brack, J. Damgård, A.S. Jensen, H.C. Pauli, V.M. Strutinsky and C. Y. Wong, *Rev. Mod. Phys.* 44:320 (1972).

52. F. Nemoto and H. Bando, *Prog. Theor. Phys.* 47:1210 (1972).

53. S. Marcos, H. Flocard and P.-H. Heenen, *Nucl. Phys.* A410:125 (1083).

54. D. Provoost, F. Grümmer, K. Goeke and P.-G. Reinhardt, *Nucl. Phys.* A431:139 (1984).

55. M. Gai, M. Ruscev, A.C. Hayes, J.F. Ennis, R. Keddy, E.C. Schloemer, S.M. Sterbenz and A.A. Bromley, *Phys. Rev. Lett.* 50:239 (1983).

56. G.A. Leander and S.E. Larsson, *Nucl. Phys.* A239:93 (1975).

57. H. Flocard, P.H. Heenen, S.J. Krieger and M. Weiss, *Prog. Theor. Phys.* 72:1000 (1984).

58. S.A.E. Johansson, *Nucl. Phys.* A22:529 (1961).

59. C. Gustafsson, P. Möller and S.G. Nilsson, *Phys. Lett.* 34B:349 (1971).

60. S. Åberg, *Nucl. Phys.* A520:35c (1990).

61. J. Dudek, T. Werner and Z. Szymański, *Phys. Lett.* 248:235 (1990).

62. W. Satula, S. Ćwiok, W. Nazarewicz, R. Wyss and A. Johnson, *Nucl. Phys.* A (1991), in press.

63. J. Höller and S. Åberg, *Z. Phys.* A336:363 (1990).

64. P. Bonche, S.J. Krieger, M.S. Weiss, J. Dobaczewski, H. Flocard and P.-H. Heenen, *Phys. Rev. Lett.* 66:876 (1991).

65. P. Bonche, S.J. Krieger, M.S. Weiss, J. Dobaczewski, H. Flocard and P.-H. Heenen, to be published.

66. S. Mizutori, Y.R. Shimizu, and K. Matsuyanagi, *Prog. Theor. Phys.* 83:666 (1990).

67. S. Mizutori, Y.R. Shimizu, and K. Matsuyanagi, *Prog. Theor. Phys.* 85:559 (1991); *Prog. Theor. Phys.* 86 (July, 1991).

68. J. Dudek, *in*: "High Spin Physics and Gamma-Soft Nuclei", J.X. Saladin, R.A. Sorensen and C.M. Vincent, eds., World Scientific, Singapore (1991) p. 146.

69. D.M. Cullen, M.A. Riley, A. Alderson, I. Ali, C.W. Beausang, T. Bengtsson, M.A. Bentley, P. Fallon, P.D. Forsyth, F. Hanna, S.M. Mullins, W. Nazarewicz, R.J. Poynter, P.H. Regan, J.W. Roberts, W. Satula, J.F. Sharpey-Schafer, J. Simpson, G. Sletten, P.J. Twin, R. Wadsworth and R. Wyss, *Phys. Rev. Lett.* 65:1547 (1990).

70. V.V. Pashkevich, *Nucl. Phys.* A169:275 (1971).

71. P. Möller, *Nucl. Phys.* A192:529 (1972).

72. R. Bengtsson, I. Ragnarsson, S. Åberg, A. Gyurkovich, A. Sobiczewski and K. Pomorski, *Nucl. Phys.* A473:77 (1987).

73. J. Blons, C. Mazur, D. Paya, M. Ribrag and H. Weigmann, *Phys. Rev. Lett.* 41:1282 (1978).

74. B. Fabbro, J. Blons, A. Greiner, J.M. Hisleour, C. Mazur, Y. Patin, D. Paya and M. Ribrag, *J. Physique Lett.* 45:L-843 (1984).

DISCLAIMER